A Hermite High–Order Finite Element for Structural Optimal Design

Luigi Morino,[1] Giovanni Bernardini,[1] Chiara Cerulli,[2] Fabio Cetta[1]

Summary

In this paper we introduce a finite–element technique based upon a three–dimensional Hermite interpolation for application to structural dynamics, within an optimal design context. The unknowns are the nodal values of the displacement, of its three partial derivatives, of its three mixed second derivatives, and of its third mixed derivative. The main advantage of such an element is the possibility of an efficient utilization of a quasi–static reduction (*i.e.*, Guyan technique), which allows one to eliminate all the degrees of freedom associated with the derivatives of the displacement field (with a reduction by a factor of 8–to–1), while maintaining a high level of accuracy. Applications include the evaluation of the natural frequencies of shell–like elastic structures, which are treated as three–dimensional objects, with only one element along the normal (comparisons with commercial–code results are included). Finally, if the nodal values of the displacement field on the two sides of the shell are expressed in terms of their semi–sum (representative of the mid–surface displacement) and their semi–difference (representative of rotation and stretching on the normal), an additional advantage is obtained by using a second Guyan reduction to eliminate the semi–differences.

Introduction

Multi–Disciplinary Optimization (MDO) denotes a methodology whereby several computer modules, each related to one of the basic disciplines may be interfaced under the umbrella of an optimizer, to yield a computer–automated optimal design of an aircraft configuration. The disciplines involved include structures, aerodynamics, aeroelasticity (*e.g.*, divergence, flutter and gust response), performance, flight dynamics, propulsion, feedback control, and aeroacoustics; the objective may be cast in terms of economic considerations (*e.g.*, life–cycle costs). This approach is particularly useful for innovative configurations, for which the designer cannot rely upon past experience (see Ref. [1] for a deeper analysis of this point).

In this paper we address a finite–element methodology for a structural MDO module. To this aim, it is useful to have an element with three major features: *(i)* it is highly desirable that the element be very flexible, so as be able to model efficiently all types of geometries (*e.g.*, plates, shells and three–dimensional elements), thereby facilitating for instance the connection of the various components (or the transition, during optimization, from one type of structure to another, *e.g.*, from thin plate to thick shell); *(ii)* it is paramount that the above feature be combined with user–friendliness, specifically, it should not require complicated topologies (requiring human intervention), thereby rendering feasible automated–resizing programming; *(iii)* last, but not least, the element should be highly accurate, so as to give good results with few elements (an important feature when repeated calculations occur, as in MDO).

The proposed element is based upon a three–dimensional Hermite interpolation, and will be referred to as the Hermite element (see Ref. [2]). The unknowns are the nodal values of the three–dimensional displacement vectors, their three partial derivatives, their three mixed second derivatives, and their third

[1]Dipartimento di Ingegneria Meccanica e Industriale, Università "Roma Tre," V. Vasca Navale 79, I–00146 Rome, Italy

[2]Aerospace Engineering/Mechanical Engineering, Delft University of Technology, Kluyverweg 1, 2629 HS Delft, The Netherlands

mixed derivative. The element satisfies the three requirements above. Specifically, in reference to Requirement *(i)*, plate/shell elements are treated as three–dimensional elements with a single element along the thickness. For Requirement *(ii)*, the topology utilized is very simple (collection of topologically hexahedral blocks, with hexahedral elements having unknowns only at the vertices; the connection at the boundary is accomplished in a very efficient manner described later). Regarding Requirement *(iii)*, it should be noted that in MDO the structural aspect that is most computer intensive is that pertaining structural dynamics (statics is an order of magnitude simpler); in view of this, methodologies that can take full advantage of quasi–static reductions (*e.g.*, Guyan's method [3]) are extremely efficient in optimal design applications. This structural–dynamics advantage is definitely the "forte" of the proposed element and stems from the fact that Guyan's quasi–static techniques may be efficiently employed within the proposed methodology, since all the derivatives may be treated as slave degrees of freedom, as they are connected to high–frequency modes, with a reduction of the number of unknowns by a factor 8–to–1. An additional quasi–static reduction is possible in the case of shells, which as mentioned above are treated like three–dimensional geometries with only one element along the normal; in this case, the nodal values of the displacement field on the two sides of the shell are expressed in terms of their semi–sum (representative of the mid–surface displacement) and their semi–difference (representative of rotation and stretching on the normal), and a second Guyan reduction is used to eliminate the semi–differences. Finally, the proposed element is not subject to the "interpolation failure" and "locking" phenomena – an indispensable requirement (see, *e.g.*, Refs. [4] and [5]; for typically used remedies, see, *e.g.*, Ref. [6]).

Hermite three–dimensional finite element

In three–dimensional analysis brick elements with linear shape functions and eight nodes are commonly employed. Serendipity high–order finite elements are also commonly used. Specifically, the twenty–node brick element has quadratic displacement shape–functions and the thirty–two–node brick element has cubic shape functions. Here, we present a feasibility study of an element based upon the third–order Hermite interpolation. This element is known as the Hermite element (see, for instance, Ref. [2], where it is also referred to as Bogner–Fox–Schmit element). This element is rarely used because of problems that arise if the domain is not topologically hexahedral. The main innovation introduced here deals with this issue and is addressed later (see Section entitled "Formulation for complex structures – a novel scheme"). First, let us discuss the element for the simple case of a topologically hexahedral domain. In particular, we want to present the advantages of the element in connection with the Guyan reduction, an aspect not sufficiently emphasized before. As mentioned above, this is crucial in the present context, of multi–disciplinary optimization (see also, Ref. [1]).

For the one–dimensional case, the Hermite interpolation, of class $\mathcal{C}^1$, is given by (in $[-1,1]$)

$$u(x) = u_1 M_1(x) + u_2 M_2(x) + v_1 N_1(x) + v_2 N_2(x), \tag{1}$$

where $u_{1,2}$ denotes the values of $u(x)$ in $x = \pm 1$, and $v_{1,2}$ denotes the values of the x–derivative of $u(x)$, $v(x) = du/dx$, in $x = \pm 1$, whereas the Hermite interpolation polynomials $M_k(x)$ and $N_k(x)$ are given by

$$M_{1,2}(x) = \frac{1}{4}(2 \mp 3x \pm x^3); \qquad N_{1,2}(x) = \frac{1}{4}(\pm 1 - x \mp x^2 + x^3). \tag{2}$$

In order to extend the concept to the three–dimensional case, introduce material curvilinear coordinates

ξ^α and consider a *brick* element, which by definition corresponds to a cube in the ξ^α–space. Using the Hermite interpolation in all three directions yields an approximation for the displacement given by

$$\mathbf{u}(\xi^\alpha) = \sum_{\mathbf{s}} P_{\mathbf{s}}(\xi^\alpha)\mathbf{u}_{\mathbf{s}} + \sum_{\mathbf{s}}\sum_{\beta=1}^{3} Q_{\mathbf{s}}^{\beta}(\xi^\alpha)\mathbf{u}_{\mathbf{s},\beta} + \sum_{\mathbf{s}}\sum_{\beta,\gamma\in I_{\beta\gamma}} R_{\mathbf{s}}^{\beta\gamma}(\xi^\alpha)\mathbf{u}_{\mathbf{s},\beta\gamma} + \sum_{\mathbf{s}} S_{\mathbf{s}}^{123}(\xi^\alpha)\mathbf{u}_{\mathbf{s},123}, \tag{3}$$

where "$_{,\alpha}$" denotes the partial derivative with respect to ξ^α (for instance $\mathbf{u}_{,\alpha\beta} = \partial^2\mathbf{u}/\partial\xi^\alpha\partial\xi^\beta$).[3] In addition, $\mathbf{s} := (s_1, s_2, s_3)$, with $s_k = 1,2$, defines the eight nodes of the brick element. Moreover, noting that the second–derivative summation spans only mixed derivatives, we have that $I_{\beta\gamma} := (1,2;2,3;3,1)$, whereas the term 123 is the only mixed third–order derivative. Finally, $P_{\mathbf{s}}(\xi^\alpha)$, $Q_{\mathbf{s}}^{\beta}(\xi^\alpha)$, $R_{\mathbf{s}}^{\beta\gamma}(\xi^\alpha)$, and $S_{\mathbf{s}}^{123}(\xi^\alpha)$ are suitable products of the Hermite polynomials in Eq. 2. For instance,

$$\begin{aligned}
P_{\mathbf{s}}(\xi^\alpha) &= M_{s_1}(\xi^1)M_{s_2}(\xi^2)M_{s_3}(\xi^3),\\
Q_{\mathbf{s}}^{1}(\xi^\alpha) &= N_{s_1}(\xi^1)M_{s_2}(\xi^2)M_{s_3}(\xi^3),\\
R_{\mathbf{s}}^{12}(\xi^\alpha) &= N_{s_1}(\xi^1)N_{s_2}(\xi^2)M_{s_3}(\xi^3),\\
S_{\mathbf{s}}^{123}(\xi^\alpha) &= N_{s_1}(\xi^1)N_{s_2}(\xi^2)N_{s_3}(\xi^3).
\end{aligned} \tag{4}$$

The expressions above yield the local interpolation procedure. The above expressions may be combined to yield a global interpolation function as $\mathbf{u}(\xi^\alpha) = \sum_p \Psi_p(\xi^\alpha) z_p$, where z_p are the unknown nodal values, whereas $\Psi_p(\xi^\alpha)$ comprises $\mathbf{u}^{(n)}$, $\mathbf{u}_{,\alpha}^{(n)}$, $\mathbf{u}_{,\alpha\beta}^{(n)}$, and $\mathbf{u}_{,123}^{(n)}$ $(n = 1,...,N)$.[4]

The problem under consideration (evaluation of the natural modes of vibration for an isotropic elastic material) may be stated as

$$\frac{1}{2}\omega^2\int_{\mathcal{V}} \rho\|\mathbf{u}\|^2 \mathrm{d}\mathcal{V} - \frac{1}{2}\int_{\mathcal{V}} \sigma^{\alpha\beta}\varepsilon_{\alpha\beta}\mathrm{d}\mathcal{V} = extr[\mathbf{u}(\xi^\alpha)], \tag{5}$$

where $\sigma_\alpha^\beta = 2G[\varepsilon_\alpha^\beta + \varepsilon_\gamma^\gamma\delta_\alpha^\beta\nu/(1-2\nu)]$ and $\varepsilon_{\alpha\beta} = (u_{\alpha/\beta} + u_{\beta/\alpha})/2$, with $..._{/\alpha}$ denoting covariant differentiation.[5] Substituting the approximation for $\mathbf{u}$ discussed in the preceding section, locally expressed by Eq. 3, yields $\frac{1}{2}\omega^2 \mathsf{z}^T\mathsf{M}\mathsf{z} - \frac{1}{2}\mathsf{z}^T\mathsf{K}\mathsf{z} = extr(\mathbf{z})$, where the vector of the unknown nodal values is given by $\mathsf{z} = \{z_n\}$, whereas the mass and stiffness matrices are respectively given by $\mathsf{M} = [m_{mn}]$ and $\mathsf{K} = [k_{mn}]$, with

$$m_{mn} = \int_{\mathcal{V}} \rho\,\Psi_m(\xi^\alpha)\cdot\Psi_n(\xi^\alpha)\mathrm{d}\mathcal{V} \qquad k_{mn} = \sum_{\alpha,\gamma}\int_{\mathcal{V}} 2G\left(P_\alpha^\gamma P_\gamma^\alpha + \frac{\nu}{1-2\nu}P_\alpha^\alpha P_\gamma^\gamma\right)d\mathcal{V}, \tag{6}$$

where $P_\alpha^\gamma(\xi^\rho) = \sum_\beta \left[\Psi_{m,\alpha}\cdot\mathbf{g}_\beta + \Psi_{n,\beta}\cdot\mathbf{g}_\alpha\right] g^{\beta\gamma}$ ($g^{\beta\gamma}$ being the contravariant metric tensor components).

[3] Throughout the paper, Greek subscripts/superscripts are used to denote curvilinear coordinates (covariant/contravariant components, or partial derivatives). Latin letters denote Cartesian coordinates.

[4] The boundary conditions considered here are either those for a free–surface boundary, which require no action (natural boundary condition), or those for a clamped–surface boundary, for which the values of the nodal displacements – and their tangential derivatives – vanish.

[5] The most general linear stress–strain relationship is given by $\sigma^{\alpha\beta} = c^{\alpha\beta\gamma\delta}\varepsilon_{\gamma\delta}$. For the sake of simplicity, this general expression is not included in this paper, since all the numerical results are limited to isotropic homogeneous material.

Validation of formulation

The above formulation is limited to topologically hexahedral structures with no discontinuities on the base vectors $\mathbf{g}^\alpha$. The extension to more general geometries is examined in the next section. In this section, we present a validation of the above formulation. Only a few test cases are presented, limited to shell–like structures, since the validation for this type of structures is critical to our claims (Requisites 1 and 3). For simplicity, for all the test cases, ρ, E and ν are constant. Thus, $\hat{\omega} = \omega\ell\sqrt{\rho/E}$ is independent of ρ, E and ℓ (where ℓ is a reference length). Our results are obtained with and without Guyan's reduction.[6] These results are compared with those obtained using an existing commercial code, ANSYS [7]. Specifically, we made the comparison with the ANSYS (two–dimensional) shell element (denoted here by *ANSYS 2D*), which is commonly used to analyze plates and shells. We also used the three–dimensional element with 20 nodes (here denoted by *ANSYS 3D 20n*), because is the most closely related to our element. To have a meaningful comparison, a consistent–mass matrix is used for all the results.

Consider first thin square plates. Let ℓ coincide with the plate edge length and τ denotes the thickness. Assume $\tau/\ell = 0.01$. The convergence analysis for the first dimensionless natural frequency, $\hat{\omega}_1 = \omega_1\ell\sqrt{\rho/E}$, of a thin square plate, free at the edges, is shown in Figs. 1 and 2. The plate is discretized with N elements along each in–plane direction and 1 element in the normal direction. Figure 1 presents the value of ω_1 as a function of $1/N$, with and without Guyan reduction. It is apparent that the Guyan reduction may be introduced with minimal penalty on accuracy, especially for finer mesh sizes. Next, we compare the results that we obtained using Guyan's reduction with those obtained using ANSYS [7]. This is shown in Figure 2, which presents $\hat{\omega}_1$ as a function of $1/DOF$, where DOF denotes the degrees of freedom.[7] The horizontal line is the frequency of the thin plate equation (eigenvalue of bi–Laplacian), obtained with the Galerkin method (with base functions given by the product of free–free beam eigenfunctions). It is apparent that our results have a higher rate of convergence, even though the ANSYS element is specifically designed for shells (the *ANSYS 3D 20n* results are not included because their convergence is too slow). Similar considerations hold for Figs. 3 and 4, where the results for a clamped plate are presented. In this case, the advantage of using Guyan's reduction is even more evident: note that the comparison is made with equal number of elements and the loss in accuracy is insignificant. The advantage of the 8–to–1 reduction in DOF (not taken into account in Fig. 3) is used in Fig. 4, where the comparison with the ANSYS results is again startling (here, we show also the results for the ANSYS three–dimensional $20-$node element).

Next, consider a spherical shell with radius $R = 5$, the length along x and y direction is 1 and the thickness is $1/100$ of this length. In this case the comparison is made just between our results with Guyan and the ANSYS two–dimensional shell. The results are presented in Figs. 5 and 6, which depict the first dimensionless frequency as a function of $1/N$ and $1/DOF$, respectively (still with $N = N_1 = N_2$, and with one element along the thickness). Similar considerations apply for this case as well.

Finally, as mentioned above, in the case of shell–like structures, it is possible to reduce the number of unknowns even further, by using a Guyan reduction a second time. Indeed, instead of the upper–

[6] In the Guyan reduction, we eliminate all the derivatives, with a reduction factor of 8–to–1. Indeed, for each value of the function, there are 7 derivatives: 3 derivatives of the first order, 3 mixed derivatives of the second order, and 1 mixed derivative of the third order.

[7] We used $1/DOF$ because the computer time for the eigen–solution is a function of DOF, and not of N; this is the key advantage of using Guyan's reduction.

and lower–side nodal displacements (u_U and u_L respectively), one may use their semi–sum and semi–difference, $u_M = (u_U + u_L)/2$ and $u_\Delta = (u_U - u_L)/2$. Since u_Δ/τ is related to thickness variations (normal components) and rotations around the mid–surface (in–plane components), the u_Δ variables correspond to high–frequency motions and therefore the Guyan reduction may be applied again.[8] The corresponding convergence analysis for a free thin plate is presented in Figures 7 and 8, which depict the first dimensionless frequency as a function of $1/N$ and $1/DOF$, respectively (again with $N = N_1 = N_2$, and with one element along the thickness).

Formulation for complex structures – a novel scheme

As mentioned above, the formulation discussed in the preceding sections (hereby referred to as the *Scheme A*) presents no problems as long as the structure is topologically hexahedral (*i.e.*, a rectangular parallelepiped in the ξ^α–space); for, in this case all the partial derivatives assume the same value for all the eight bricks that share a node. Major problems arise for more complex structures, even for structures that may be obtained as combinations of topologically hexahedral substructures, which is the only case considered here. We will refer to these substructures as *blocks* (each block is divided into $N_1 \times N_2 \times N_3$ *bricks*). Specifically, problems arise when the coordinate lines of two adjacent blocks present a discontinuity (specifically, when the covariant base vectors, $\mathbf{g}_\alpha = \partial \mathbf{x}/\partial \xi^\alpha$, are not continuous). In this case, the partial derivatives of any function f with respect to ξ^α are discontinuous (recall $\partial f/\partial \xi^\alpha = \mathbf{g}_\alpha \cdot \mathrm{grad}\, f$). As far as the first–order derivatives are concerned, if the gradient is continuous the problem is removed by assuming as unknowns the values of the Cartesian coordinates of $\mathrm{grad}\,\mathbf{u}$, $u_{k,h} = \partial u_k/\partial x_h$); these quantities are continuous under the present assumption of continuity for E and ν. The partial derivatives may then be obtained as $\partial f/\partial \xi^\alpha = \mathbf{g}_\alpha \cdot \mathrm{grad}\, f$. The problem, however, remains for the second–order derivatives, because, in order to express them in terms of Cartesian components, one needs all the second–order derivatives, not only the mixed ones. Similar considerations hold for the third–order derivatives. In order to address these issues, several approaches have been explored and presented in Ref. [8]. The first approach tried in Ref. [8] consists of expressing the second– and third–order derivatives, via suitable finite differences, in terms of the function at the nodes (akin to the approach used by Gennaretti *et al.* [9] in a related boundary–element method for aerodynamics). The results for a topologically hexahedral structure (unconstrained plate with thickness ratio of $1/100$), are much worse that those obtained with Scheme A discussed above, and even worse than those obtained with the NASTRAN CHEXA element (Ref. [6]). In another approach used in Ref. [8], the second and third order derivatives were set equal to zero. The results were even worse. Then, still in Ref. [8], in order to identify the source of the problem, only the third order derivative were set equal to zero; obviously this attempt would not have resolved the problem of the second–order derivatives – nonetheless, the results were not very good. This suggested that the problem lies with the second–order (and not the third–order) derivatives. This led to the idea of introducing a fifth–order Hermite interpolation, because in this case all the second–order derivatives are available and hence they as well may be expressed in terms of Cartesian second–order derivatives (for, the second–order derivatives with respect to ξ^α are the covariant components of the Hessian tensor). This shifts the problem from the mixed second– and third–order derivatives into those of order 3, 4 and 5. As expected, the results obtained with the full fifth–order scheme (*i.e.*, a fifth–order extension of Scheme A) were much better than the corresponding third–order ones. However, those obtained with the modified fifth–order scheme (*i.e.*, by setting to zero the derivatives of order 3, 4, and 5) were not as good as hoped (for a coarse grid, this scheme behaves worse than the third-order Scheme

[8] This could be interpreted as a discrete implementation of the Kirchhoff shell hypothesis.

A).

On the basis of these somewhat disappointing results, a new scheme has been explored and the results are presented here. In this scheme (hereby referred to as *Scheme B*), the second– and third–order derivatives are treated as independent variables for each element of a given node (*i.e.*, for each node, the second– and third–order derivatives are allowed to assume eight different values). Of course, Scheme B requires many more variables than Scheme A. Hence, as a compromise, we introduced the novel scheme announced above (hereby referred to as *Scheme C*, which is a combination of the other two. Specifically, as stated in the beginning of this section the structure is assumed to be composed of blocks (*i.e.*, topologically hexahedral structures), and in the proposed Scheme C, the Scheme B approach is used for the block–boundary nodes (*i.e.*, nodes that are common to two or more blocks), and Scheme A is used for all the interior nodes (*i.e.*, for the large majority of the nodes). In order to validate this scheme, we analyzed a thin plate like the one presented in Figures 1 and 2. Here, the plate is artificially divided into two halves, and each of the two resulting plates is treated as a different block. Thus, for the same plate we can use three schemes: (a) Scheme A (as in Figs. 1 and 2), (b) Scheme B (in which each brick is considered as a separate block, and (c) Scheme C in which each of the two portion is treated as a separate block. In Fig. 9 we present the first twenty frequencies obtained using the three different schemes for analyzing this structure. With *Kode 0–0* we denote Scheme A for all the plate (this is the same approach used in the preceding sections), whereas with *Kode 1–0* and *Kode 1–1* we denote Schemes C; and Scheme B, respectively. One may note that these results are quite satisfactory.

In summary, the method is very promising, but further analysis is warranted. Specifically, more extensive applications are needed. In particular, more complicated geometries should be examined. Also, higher order schemes (*i.e.*, the fifth order one) should be analyzed.

Reference

1. Morino, L., Bernardini, G., Mastroddi, F., "Multidisciplinary Optimization for the Conceptual Design of Innovative Aircraft Configurations," ICCES'04, Madeira, Portugal, 16–19 July 2004.
2. Chen, G., Zhou, J., "Boundary Element Methods," Academic Press, p.176, 1992.
3. Guyan, R. J., "Reduction of Stiffness and Mass Matrices," *AIAA Journal*, Vol. 3, No. 2, 1965.
4. Brenner, S. C., Scott, L. R., "The Mathematical Theory of Finite Element Methods," Springer–Verlag, 1996.
5. Braess, D., "Finite Elements: Theory, Fast Solvers, and Applications in Solid Mechanics," Cambridge University Press, 1997.
6. Macneal, R. H., "Finite Elements: Their Design and Performance," Marcel Dekker, Inc., 1994.
7. Anonimous, "Introduction to ANSYS," ANSYS, Release 5.5, ANSYS Inc., 1998.
8. Morino, L., Mastroddi, F., Bernardini, G., and Piccirilli, M., "A Hermite–interpolation finite element for structural dynamics," *XVI Congresso Nazionale AIDAA* Palermo, 24–28 Settembre 2001.
9. Gennaretti, M., Calcagno, G., Zamboni, A., and Morino, L., "A high order boundary element formulation for potential incompressible aerodynamics," *The Aeronautical Journal*, Vol. 102, No. 1014, pp. 211–219, 1998.

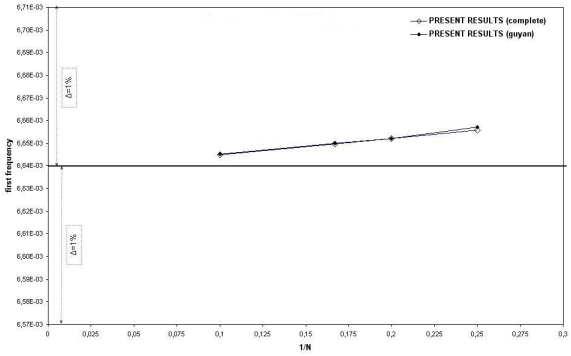

Figure 1: Free square plate: $\hat{\omega}_1$ *vs* $1/N$

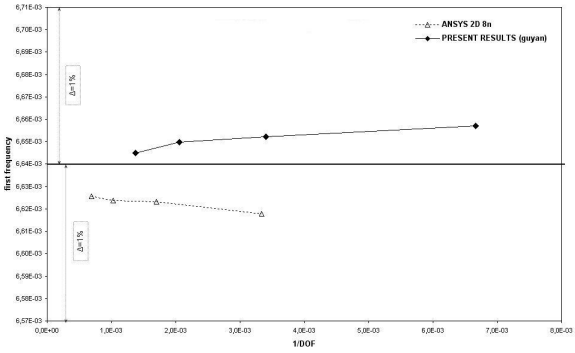

Figure 2: Free square plate: $\hat{\omega}_1$ *vs* $1/DOF$

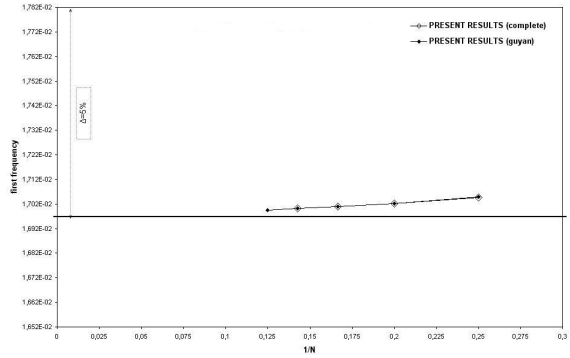

Figure 3: Clamped square plate: $\hat{\omega}_1$ vs $1/N$

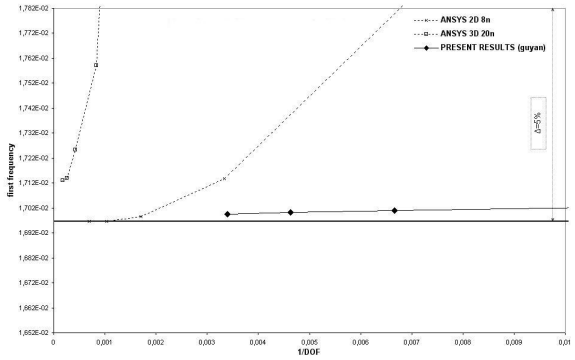

Figure 4: Clamped square plate: $\hat{\omega}_1$ vs $1/DOF$

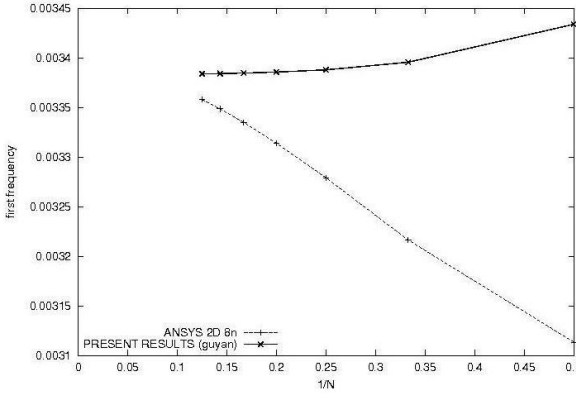

Figure 5: Free spherical shell: $\hat{\omega}_1$ *vs* $1/N$

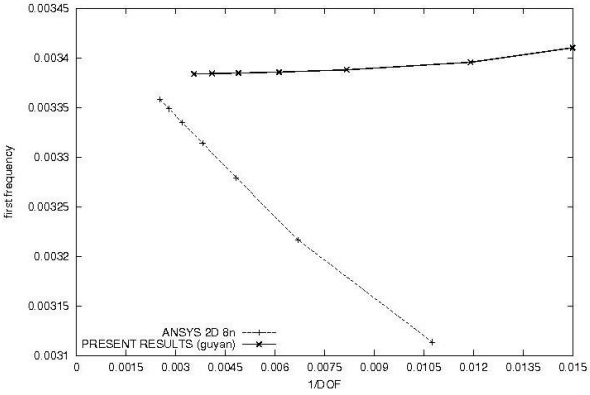

Figure 6: Free spherical shell: $\hat{\omega}_1$ *vs* $1/DOF$

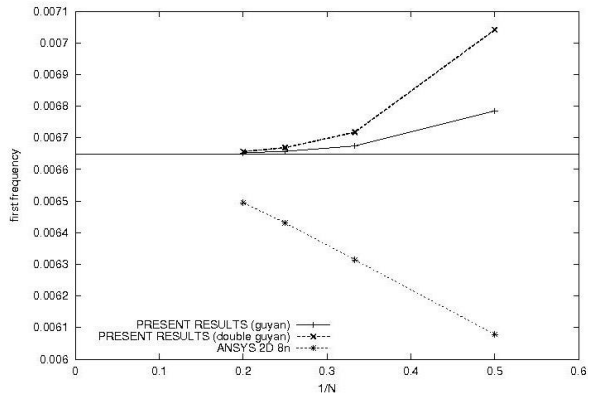

Figure 7: Double Guyan. Free square plate: $\hat{\omega}_1$ *vs* $1/N$

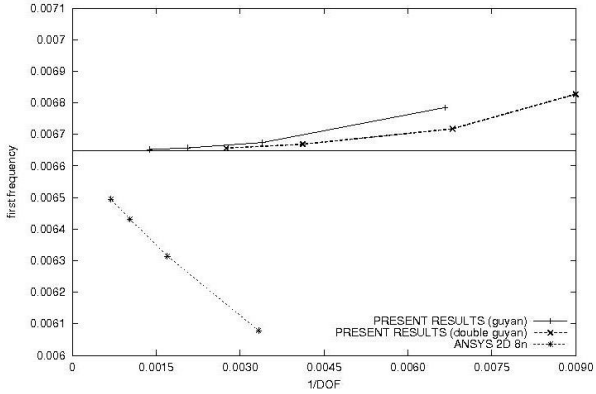

Figure 8: Double Guyan. Free square plate: $\hat{\omega}_1$ *vs* $1/DOF$

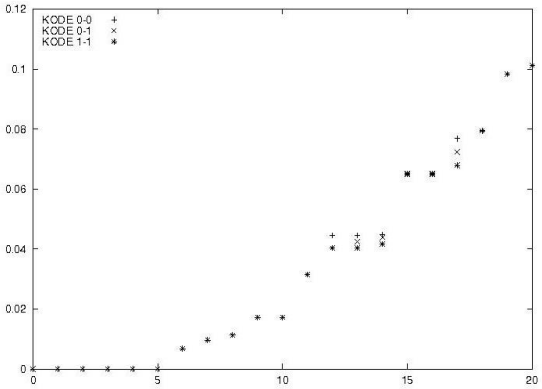

Figure 9: Free square plate: first twenty natural frequencies.